8118 *Macromolecules* **2009**, *42*, 8118–8128
DOI: 10.1021/ma901552a

Macromolecules
ARTICLE

Factors Affecting the Formation of the Monomer Sequence along Styrene/Methyl Methacrylate Gradient Copolymer Chains

Lin Wang and Linda J. Broadbelt*

Department of Chemical and Biological Engineering, Northwestern University, Evanston, Illinois 60208

Received July 16, 2009; Revised Manuscript Received October 1, 2009

ABSTRACT: The impact of the synthesis conditions on the formation of the monomer sequences of styrene (S) and methyl methacrylate (MMA) gradient copolymers synthesized by forced gradient copolymerization with nitroxide-mediated controlled radical polymerization (NM-CRP) was investigated using kinetic Monte Carlo (KMC) simulations. The factors affecting the formation of the individual segments, arrangement of these segments along the chain, and the uniformity of monomer sequences were investigated. It was shown that instantaneous segment lengths increase exponentially as a function of monomer composition. The concentration of nitroxyl radicals also plays a key role in the formation of segment lengths. In addition, the arrangement of the segments mainly depends on the feed profile of the second monomer. A constant feed profile, which is widely used in current syntheses of gradient copolymers, is shown to not be suitable to make a structural gradient along the chain. It was also demonstrated that the uniformity of sequence patterns can be affected by the entire growth history of the chains, and thus strong control over the uniformity of chain growth is required throughout the reaction in order to achieve sequences in different chains that resemble one another.

Introduction

Linear block copolymers, which are typically comprised of two or more chemically distinct polymer blocks, have been used in a wide range of applications because the local segregation of different polymer blocks can yield microphase structure of nanometer size.[1,2] Traditionally, block copolymers are prepared by living anionic polymerization, which restricts the block copolymers that can be synthesized to a limited range of comonomer pairs and architectures. The introduction of living radical polymerization (LRP), which also has a degree of livingness yet is much more flexible than living anionic polymerization, has made it possible to "tune" the sequence pattern along the copolymer chains by proper choice of both monomer type and synthesis recipe.[3] On the basis of this synthesis technique, a relatively new class of copolymers, gradient copolymers, was introduced.[4] Gradient copolymers are expected to have an intermediate microscopic chain structure between block copolymers and random copolymers.[5] As depicted in Scheme 1, the most appealing feature of this chain microstructure is that segments comprising the chain vary in length according to a certain pattern from one end to the other. It has been theorized that gradient copolymers can undergo microphase separation like block copolymers and offer a larger degree of control over the interfacial profile than block copolymers of the same composition, which may lead to a wide range of applications.[6−8] It has been reported that the interfacial behavior of gradient copolymers can be significantly affected by their monomer sequence along the chain.[8−11]

Despite the important role that monomer sequence plays, the explicit monomer sequence along the chain is still elusive for most synthesized gradient copolymers reported in the literature because of the difficulties in measuring monomer sequence directly by current experimental techniques and the limited capacity of conventional simulation techniques, such as continuum models and statistical models, to report the temporal evolution of monomer sequence of the entire population of diverse chains.[3,12,13] In fact, structural information on gradient copolymers is studied only at the level of a compositional gradient, which is the variation of local copolymer composition along the chain. The existing synthesis methods for gradient copolymers have been developed based on the criterion that instantaneous composition, F_{inst}, or cumulative composition, F, varies monotonically and continuously as a function of chain length.[3] Clearly, the explicit monomer sequence along the chain would be a more definitive criterion to characterize gradient copolymers.

Currently, LRP is the best synthesis method to prepare gradient copolymers. Because the lifetime of the majority of propagating radicals is much longer in LRP than in conventional free radical polymerization (FRP), it is possible to vary the monomer composition in a predetermined manner during the growth of a chain.[3] The variation of the monomer composition in a reaction system can be realized by composition drift, which is called spontaneous gradient copolymerization, or by the addition of the second monomer, which is referred to as forced gradient copolymerization. In this work, we only focused on studying synthesis conditions in forced gradient copolymerization because it can be applied to a wider range of comonomer pairs than spontaneous gradient copolymerization.[14] For forced gradient copolymerization via LRP, the following factors are typically adjusted for a given reaction system to design the synthesis recipes for gradient copolymers: the feed profile of the second monomer, the concentration of the unimolecular initiator, and, in some cases, the addition of free nitroxyl radicals.

Adjusting the feed profile is the most widely used approach to vary the sequence along gradient copolymer chains. For instance, Min et al. showed by experiment that the *n*-butyl acrylate/*tert*-butyl acrylate (nBA/tBA) comonomer distribution along the chain can be influenced by adjusting the feed rate of the second monomer.[15] Recently, Mok et al. prepared styrene/4-acetoxystyrene (S/AS) gradient copolymers with different compositional

*To whom correspondence should be addressed. Phone: (847) 491-5351. E-mail: broadbelt@northwestern.edu.

 Published on Web 10/13/2009

Scheme 1. Schematic Representation of the Composition in Block, Gradient, and Random Copolymers[a]

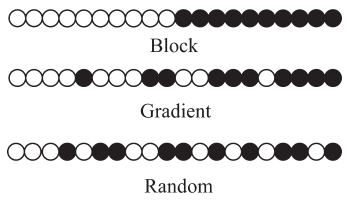

[a] The open circles denote monomer A, and the closed circles denote monomer B.

gradients along the chain by varying the feed profile during the reaction.[16] The concentration of initiator is usually tuned in order to achieve a narrow distribution of molecular masses in the population while still maintaining a reasonable reaction rate. A low polydispersity index of molecular weight (molecular weight PDI) is typically considered to denote high uniformity of chain growth during the reaction, which is essential to achieve sequence patterns in different chains that resemble each other.[3] In addition to the initiator, extra free nitroxyl radicals are necessary in order to maintain the reaction as living in the NM-CRP involving methacrylic esters because NM-CRP provides a very poor degree of control over their polymerization.[1]

Although experimental efforts can help direct the optimization of synthesis recipes, simulations promise to be even more illuminating for the design of synthesis recipes because they can provide more details about the monomer sequence along the chain. To that end, there are several theoretical studies aimed at optimizing compositional gradients. Continuous models have been used to simulate a semibatch process with reversible addition−fragmentation transfer radical polymerization (RAFT) and optimize the feed profile in order to achieve a targeted linear compositional gradient copolymer, in which F_{inst} and average chain length, DP_n, have a linear relationship.[17,18] In addition, several equation-based models were developed and utilized to study the optimal synthesis conditions to achieve a linear compositional gradient.[19,20]

Recently, we reported a simulation framework based on kinetic Monte Carlo (KMC), which can predict the explicit sequence formed along each chain by tracking the growth of each individual chain instead of concentration.[21,22] From the monomer sequence information on each chain, the overall picture of the monomer sequence along the chain in the entire population can be further mapped according to the variation of the number-average segment length along the chain, where the local number-average segment length is the mathematical average of all the segment lengths formed at the same normalized chain location. One of the striking features that KMC simulations revealed is that the variation in segment lengths can be rather minor even if there is a significant change in composition along the chain. This finding suggests that the current understanding of which synthesis strategies achieve compositional gradients may not necessarily be applied to prepare well-defined monomer sequences along the chain.

To the best of our knowledge, no specific efforts have been made to investigate the factors affecting the formation of monomer-by-monomer sequence in a copolymerization system, except for very short chains.[23] Here, we utilized KMC simulations to investigate the influence of different synthesis conditions on the formation of monomer sequence along the chain in S/MMA forced gradient copolymerization with BlocBuilder as the unimolecular initiator using NM-CRP. The synthesis conditions that were studied included the feed profile of the second monomer, initiator concentration, and addition of free nixtroxyl radicals. The factors that affect the formation of individual segments, the monomer sequence along the chain, and the uniformity of monomer sequences in different chains are discussed.

Simulation Methodologies

KMC Framework. The "Monte Carlo step" is determined by a direct, rejection-free algorithm, in which the reaction occurring at a specific instant is determined stochastically based on reaction probabilities:[22]

$$\sum_{v=1}^{\mu-1} P_v < r_1 < \sum_{v=1}^{\mu} P_v \tag{1}$$

where μ is the index of the selected reaction channel, P_v is the probability of the vth reaction channel, and r_1 is a random number uniformly distributed between 0 and 1. The probability for each reaction is determined based on its fraction of the total rate of reaction.

$$P_v = \frac{R_v}{\sum_{v=1}^{M} R_v} \tag{2}$$

Here, R_v is the stochastic rate of the vth reaction, which is defined by

$$R_v = c_v h_v \tag{3}$$

where h_v is the product of the numbers of molecular reactants involved in the vth reaction that are present at that moment and c_v is the reaction parameter based on the number of distinct molecules. c_v can be determined by the more familiar reaction rate constant, k_v, which is based on concentration of reactants in the system. For monomolecular reactions, k_v and c_v are equal; for bimolecular reactions, c_v equals k_v divided by volume, V; for trimolecular reactions, c_v equals k_v divided by V^2. The model was developed based on elementary reactions including initiation, propagation, termination, and combination/dissociation with nitroxyl radicals, as described in our earlier work.[21] Kinetic parameters, k_v, for all of the reactions included are reported in Table 1.

The time interval between reactions is determined by

$$\tau = \frac{1}{\sum_{v=1}^{M} R_v} \ln\left(\frac{1}{r_2}\right) \tag{4}$$

where r_2 is a second random number uniformly distributed between 0 and 1. The random numbers r_1 and r_2 were determined by a pseudorandom number generator provided in the C standard general utilities library with execution time as the seed. Radical chains and dormant chains were subdivided according to their ultimate and penultimate units: M−M*, M−S*, S−S*, S−M*, M−M−SG1, M−S−SG1, S−S−SG1, and S−M−SG1, where SG1 is the nitroxyl radical, in order to incorporate differences in reactivity of different chain ends, including penultimate effects on propagation reactions between propagating radicals and monomers as well as decoupling, into the model.

On the basis of the algorithm above, the KMC simulation framework was written in house. In order to validate the random selection procedure of reactions, internal consistency tests were conducted, i.e., to check whether the frequency of occurrence of a certain reaction during the KMC simulation matched the theoretical probability determined by the fraction of its reaction rate of the total reaction rate. The internal consistency test revealed that there was an excellent match between these two values for all the possible reactions in our system.

Table 1. Kinetic Parameters Used in MMA/S KMC Simulations

reactions	frequency factor, A (s^{-1}, L mol^{-1} s^{-1} or L^2 mol^{-2} s^{-1})	activation energy, E_a (kcal/mol)
initiator dissociation[24]	2.4×10^{14}	26.84
initiator radical addition to S monomer[25,a]	3.16×10^{7}	2.44
initiator radical addition to MMA monomer[25,a]	1.0×10^{9}	0.62
thermal initiation of S monomer[26]	6.3×10^{5}	27.44
homopropagation of MMA-terminated radical chains[27,b]	2.67×10^{7}	5.35
homopropagation of S-terminated radical chains[28,b]	4.27×10^{7}	7.76
disproportionation between MMA-terminated radical chains[29,30,c,d]	8.16×10^{8}	2.84
combination between MMA-terminated radical chains[29,30,c,d]	5.44×10^{8}	2.84
disproportionation between S-terminated radical chains[31,d]	4.31×10^{8}	1.5
combination between S-terminated radical chains[31,d]	2.45×10^{9}	1.5
chain transfer to MMA monomer[32,e]	2.67×10^{2}	5.35
chain transfer to S monomer[33]	2.31×10^{6}	12.67
decoupling of M−M−SG1[1]	2.4×10^{14}	24.86
decoupling of S−M−SG1[1]	2.4×10^{14}	25.81
decoupling of M−S−SG1[1]	2.4×10^{14}	27.49
decoupling of S−S−SG1[1]	2.4×10^{14}	29.88

reactions	rate coefficient (L mol^{-1} s^{-1})
coupling of initiator[34,f]	2.0×10^{6}
coupling of MMA-terminated radical chains[35,g]	4.0×10^{4}
coupling of S-terminated radical chains[36,f]	4.75×10^{5}

[a] The addition rate constants of initiator radical to S and MMA monomers were determined by the experimental data of the primary radical $(CH_3)_2\dot{C}OH$ with S and MMA monomers. [b] Penultimate reactivity ratios were obtained from the work of Fukuda et al. as $r_{11} = r_{21} = 0.523$, $r_{22} = r_{12} = 0.46$, $s_1 = 0.3$, $s_2 = 0.53$, in which monomer 1 is S and monomer 2 is MMA.[37] [c] Determined by the disproportionation/combination ratio k_{td}/k_{tc} of MMA-terminated radical chains.[30] [d] The rate constants of cross-termination reactions between MMA-terminated radical chains and S-terminated radical chains were determined as the geometric mean of the homotermination reaction rate coefficients. [e] Determined by k_{tr}/k_p value.[32] [f] Determined by extrapolation from the experimental data. [g] Weakly dependent on temperature, so an average value over the temperature range of 10−50 °C was used.

Table 2. Deviation of Simulated Results with Different Sample Sizes Varying between 10^9 and 10^{10} Initial Monomers

property, x	$\lvert(x-\bar{x})/\bar{x}\rvert_{avg}$	$\sigma_{\lvert(x-\bar{x})/\bar{x}\rvert}$
M_n	0.000 713	0.000 877
M_w	0.000 019	0.000 014
F	0.000 012	0.000 014
f	0.000 014	0.000 023
conversion	0.000 762	0.000 948

In order to determine the sample size that is necessary to ensure convergence of the KMC simulations, we varied the number of monomer molecules that were initialized in the reaction system at the beginning of the simulation between 10^9 and 10^{10}, which is sufficient to generate 10^6−10^7 radical chains in the reaction system. Under the same reaction conditions, the most important properties of polymerization, including M_n, M_w, conversion, overall copolymer composition, F, and monomer composition, f, were simulated with 10 different initialized sample sizes between 10^9 and 10^{10}. The mean value of a certain property, $\bar{x}$, was calculated based on all the simulated results of different initialized sample sizes. The deviation of a simulated property predicted with a certain initialized sample size, x, from the mean value of this property, $\bar{x}$, was expressed as $|(x-\bar{x})/\bar{x}|$. Table 2 lists the average deviation from the mean value when the sample size is varied from 10^9 to 10^{10}, $|(x-\bar{x})/\bar{x}|_{avg}$, as well as the standard deviation in these samples, $\sigma_{|(x-\bar{x})/\bar{x}|}$. The simulated results for different samples sizes between 10^9 and 10^{10} show negligible differences. Since computational time increases dramatically with increasing sample size from 10^9 to 10^{10}, 10^9 monomer molecules were initialized in all simulations in this work.

Characterization of Monomer Sequences. The explicit monomer sequence of each chain was tracked by recording the length of each individual segment, which is the number of repeating units comprising the segment, in sequence from the initiation of the chain to the end of reaction or the termination of the chain.[21] In order to correlate the segment lengths to their locations on a given chain, a normalized chain location was assigned to each segment on the chain. In this way, the monomer sequence of each chain was mapped by plotting the variation of segment lengths as a function of the normalized chain location. The overall picture of the monomer sequences extracted from the entire population was then further mapped according to the variation of the average segment lengths as a function of normalized chain location. In addition, the uniformity of monomer sequences formed in different chains was characterized in detail by the local segment PDI along the chain.

Instantaneous Average Segment Lengths. In addition to these explicit measures of monomer sequence as a function of chain length, we also monitored the average segment lengths formed at a given instant. The relationship between the segment lengths formed at a given instant and the operating conditions, such as monomer composition, provides a straightforward basis to design a recipe in order to achieve a targeted monomer sequence along the chain. In order to unravel these relationships, we investigated the instantaneous segment lengths formed under different reaction conditions, such as monomer composition and concentration of nitroxyl radicals. The instantaneous segment lengths of S and MMA, $N_{inst,S}$ and $N_{inst,MMA}$, are the average segment length formed at a given instant calculated as follows:

$$N_{inst,i} = \frac{dM_i}{dn_i} \tag{5}$$

where dM_i is the amount of monomer i incorporated into copolymer chains at any instant and dn_i is the number of segments to which dM_i was added at that instant.

In FRP, the development of the segments can be considered to be instantaneous because propagation is fast, and thus dn_i is equal to the increase in the number of segments of monomer i. However, in LRP, the growth of segments at a given instant does not necessarily result in an increase in the number of segments. Because the transient lifetime of a

Table 3. Simulation Conditions for S/MMA Gradient Copolymerization[a]

simulations	$[I]_0$,[b] mol L^{-1}	$[SG1]_0$, mol L^{-1}	initial amount of S, mL	initial amount of MMA, mL	type of fed monomer/ total amount, mL	feed profile of monomer, mL h^{-1}	feed profile of SG1, mol h^{-1}
MS1	0.01	0	5	0	MMA/60	7.5	1.4×10^{-4}
MS2	0.01	0	5	0	MMA/20	2.5	0
MS3	0.1	0	5	0	MMA/20	2.5	0
MS4	0.01	0.05	5	0	MMA/20	2.5	0
MS5	0.01	0.05	5	0	MMA/4	0.5	0
MS6	0.01	0.05	5	0	MMA/60	7.5	0
MS7	0.01	0	5	0	MMA/20	2.5	4.7×10^{-5}
MS8	0.01	0	5	0	MMA/40	5	9.4×10^{-5}
MS9	0.01	0	5	0.23	MMA/80	1 (0−5.5 h)[c] 22.5 (5.5−8 h)	1.9×10^{-5} (0−5.5 h)[c] 4.19×10^{-4} (5.5−8 h)
MS10	0.01	0.004	5	0	MMA/20	2.5	4.7×10^{-5}
MS11	0.01	0.004	5	0	MMA/20	2.5	1.18×10^{-4}

[a] In all the simulation runs, the reaction temperature was fixed at 95 °C and the reaction time was 8 h. [b] BlocBuilder was used as the unimolecular initiator. [c] 8 mL of MMA and 1.49×10^{-4} mol of SG1 were added all at once at 5.5 h of reaction for a quick transition from an S-dominant to an MMA-dominant reaction environment.

Table 4. Material Properties of Simulation Runs after 8 h of Reaction Time

simulations	M_n, g/mol	M_w, g/mol	DP_n	PDI	F_S	F_{MMA}	conversion, S, %	conversion, MMA,%
MS1	164 000	210 300	1628	1.28	0.16	0.84	30.0	11.1
MS2	145 000	243 000	1429	1.68	0.34	0.66	45.8	19.6
MS3	33 000	45 000	326	1.36	0.27	0.73	92.5	59.6
MS4	26 000	31 800	256	1.2	0.32	0.68	10.5	4.8
MS5	2 600	3 500	25	1.3	0.63	0.37	2.0	1.3
MS6	201 300	228 400	1999	1.13	0.15	0.85	35.8	14.9
MS7	94 700	132 000	933	1.4	0.33	0.67	32.3	14.5
MS8	140 000	184 700	1386	1.32	0.22	0.78	32.6	13.1
MS9	50 000	65 400	492	1.33	0.35	0.65	2.5	0.3
MS10	101 500	126 600	1001	1.24	0.32	0.68	35.5	16.6
MS11	22 000	26 430	217	1.2	0.35	0.65	9.5	3.8

radical, i.e., the time interval between activation and deactivation of a radical is very short in a successful LRP, the growth of a segment can be arrested by deactivation before it is fully developed by a cross-propagation or termination event and can be resumed by propagation at a later stage of reaction. When addition of monomer *i* is strongly favored, homopropagation of this type of monomer is highly preferred. Under this circumstance, it is likely to have only homopropagation during a cycle of activation for a radical with monomer *i* as the ultimate unit. Compared to the transient lifetime, the cycle of deactivation/reactivation of the same radical is much longer. Thus, a significant amount of monomer can be incorporated into copolymers without changing the total number of segments over a short period of reaction (dM_i is increased, but dn_i remains the same). This is more likely to occur in the system when the concentration of capping agent is high and the homopropagation of one type of monomer is highly favored. In this case, the instantaneous segment length can be overestimated if dn_i is considered to be merely equal to the increase in the number of segments of monomer *i* without taking into account the history of the chain. Therefore, in living radical polymerization, the instantaneous segment length, i.e., the average segment length of one type of monomer formed during a short time interval, should include not only the completed segments but also the segments under development. The KMC framework enables the prediction of the growth of each individual chain and thus allows the amount of monomer that is incorporated onto copolymer chains at any instant and the number of segments to which the monomers are attached to be explicitly tracked no matter whether the segments are completed within this short period of time.

The formation of segments in LRP can be significantly affected by the reversible activation/deactivation procedures of radicals, which is quite different from FRP where the formation of segments is simply a function of reactivity ratios and monomer composition at that instant. Therefore, mathematical models which are aimed at predicting instantaneous segment length in FRP[12] cannot be applied in LRP in many cases.

Results and Discussion

Structural gradient copolymers are distinguished from random copolymers and block copolymers by a gradual change in segment lengths along the chain. Scheme 1 depicts an ideal monomer sequence for a structural gradient copolymer, where the segment length of monomer A decreases while that of monomer B increases gradually as the chain grows longer. Finally, the segment length of monomer B at the tail is increased to be equal in length to that of monomer A at the head of the chain.

Thus, in tuning the synthesis conditions in forced gradient copolymerization with LRP, this "optimal" monomer sequence along the chain was used as a target. Reaction conditions that can be controlled in a facile way during the synthesis in practice were varied, and the particular variables and their values are summarized in Table 3. The overall material properties of copolymers synthesized from each recipe including M_n, M_w, and PDI that were predicted from the KMC simulations are listed in Table 4. By comparing the differences in the monomer sequence obtained from different reaction conditions, we summarized the impact of reaction conditions on the formation of sequences based on the following characteristics: the formation of individual segments, the variation of the segment lengths along the chain, and the polydispersity of monomer sequences formed in different chains.

Validation of the KMC Models for S/MMA Copolymerization with the Presence of Free Nitroxyl Radicals. The KMC models for S/MMA forced gradient copolymerization with BlocBuilder as the initiator were validated against the experimental data measured in our laboratory, and the details of this work were reported elsewhere.[21] However, we did not perform experiments in which the free nitroxyl radical (SG1)

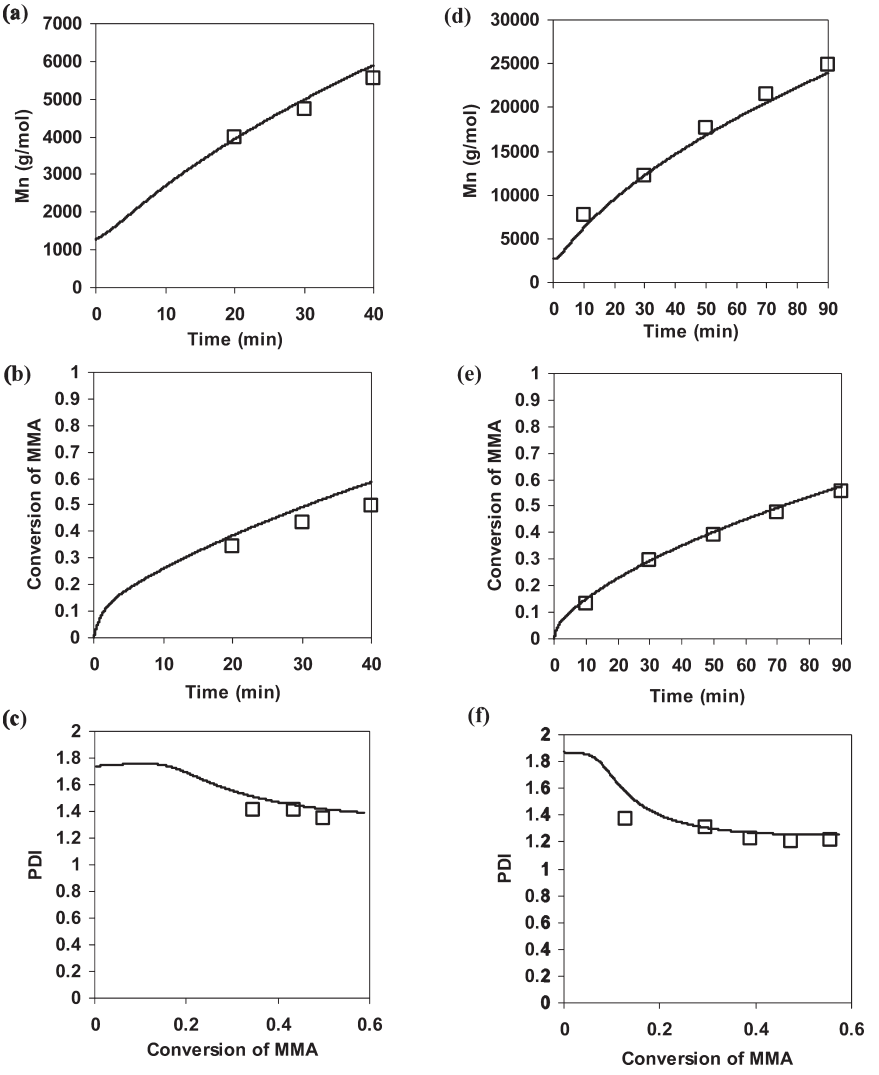

Figure 1. Simulation results (solid lines) and experimental results (open squares; Nicolas et al.[1]) of the evolution of M_n, conversion of MMA monomer, and polydispersity index (PDI) as a function of reaction time. (a, b, c) P2 which is prepared by mixing 0.8 mol of MMA, 0.077 mol of S, 1.03×10^{-2} mol of BlocBuilder, and 1.04×10^{-3} mol of SG1 reacting at 90 °C. (d, e, f) P3 which is prepared by mixing 1.2 mol of MMA, 0.116 mol of S, 3.74×10^{-3} mol of BlocBuilder, and 4.39×10^{-4} mol of SG1 reacting at 90 °C.

was added in this earlier work. In the present work, free SG1 is needed to impart control in some simulation runs where the monomer composition strongly favors MMA. In order to verify the capacity of the KMC models to predict reactions involving free SG1, we conducted simulation runs according to the synthesis recipes reported in the literature in which free SG1 was added in the beginning of the reaction.[1] As shown in Figure 1, the KMC simulations were able to capture the evolution of M_n and conversion rate of MMA as a function of reaction time, and the evolution of polydispersity as a function of conversion for two different experimental runs very well.

Formation of Individual Segments. Control of the formation of each individual segment is the key to achieve a predesigned sequence pattern along the chain. Through the KMC simulations, it was demonstrated that the formation of individual segments in the copolymerization of S/MMA with NM-CRP can be affected not only by the monomer composition in the reaction system but also by the concentration of nitroxyl radicals. The effects of these two variables are discussed in the following sections.

a. Relationship between Monomer Composition and Instantaneous Average Segment Lengths. Figure 2 shows the evolution of the instantaneous average segment lengths of S and MMA, $N_{inst,S}$ and $N_{inst,MMA}$, as a function of monomer composition in MS1, where f_{MMA} increases from 0.03 at the beginning of the reaction to 0.95 at the end of the reaction.

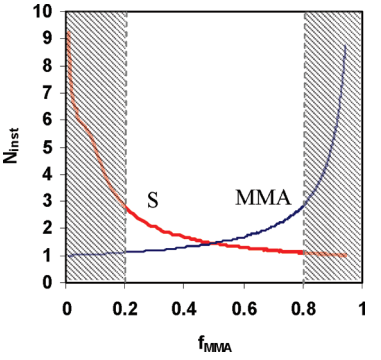

Figure 2. Evolution of instantaneous average segment length of MMA and S, $N_{inst,MMA}$ and $N_{inst,S}$, as a function of MMA monomer composition, f_{MMA}, in MS1. The regions where the segment lengths can be varied efficiently by changing the monomer composition are shaded.

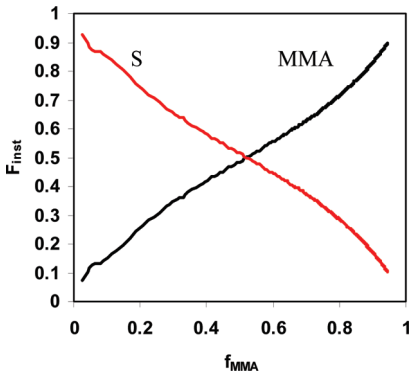

Figure 3. Evolution of instantaneous copolymer composition of MMA and S, $N_{inst,MMA}$ and $F_{inst,S}$, as a function of MMA monomer composition, f_{MMA}, in MS1.

In this reaction, $N_{inst,MMA}$ increases while $N_{inst,S}$ decreases as the chains grow longer. However, the segment lengths of a given monomer change surprisingly slowly when the composition of the same type of monomer is less than 0.8. For instance, $N_{inst,MMA}$ is increased from 1 to only 3 when f_{MMA} is increased from 0.03 to 0.8. This presents a stark contrast to the variation of the instantaneous copolymer composition as a function of monomer composition, in which $F_{inst,MMA}$ and $F_{inst,S}$ increase continuously and almost linearly as a function of monomer composition, as shown in Figure 3.

The KMC simulations reveal that the instantaneous average segment lengths for both monomers actually increase exponentially with increasing monomer composition in the S/MMA copolymerization system. When a S/MMA reaction system does not strongly favor one monomer, only very short segments can be formed and incorporated into the chain. In fact, this exponential relationship between instantaneous average segment length and monomer composition is generalizable for comonomer pairs whose reactivity ratios are all less than one. In this case, the propagating radicals prefer to react with monomers of the type different from their ultimate units, which makes it difficult to achieve continuous homopropagation between propagating chains and monomers of the same type as their ultimate units without interruption by cross-propagation. Therefore, long segments can only be formed when the monomer composition strongly favors one monomer and cross-propagation can be suppressed to a great degree. This observation is consistent with the traditional copolymerization kinetic theory that significant segment lengths can be formed only by strongly increasing the composition of the same type of monomer when reactivity ratios are similar.

When segments are short, a small change in the segment lengths can lead to a large change in the instantaneous copolymer composition. For instance, $N_{inst,MMA}$ and $N_{inst,S}$ are both 1 unit long with f_{MMA} equal to 0.5. When f_{MMA} is increased to 0.8, $N_{inst,MMA}$ is increased to 3 and $N_{inst,S}$ remains unchanged. There is no marked difference in the microscopic chain structures when two-unit long MMA segments are connected with one-unit long S segments compared to alternating monomer sequences where all the segments are one unit long. Thus, although a significant compositional gradient is formed with $F_{inst,MMA}$ varied from 0.5 to 0.8, the monomer sequence does not change dramatically as measured by the monomer segment lengths.

These results suggest that a structural gradient, in which segment lengths vary according to a predesigned manner along the chain, can only be achieved in a relatively narrow region of monomer composition which is marked as the shadowed portion in Figure 2. Outside of this monomer composition region, only very short segments of S and MMA can be incorporated into the chain, which results in monomer sequences resembling that of random copolymers. Within this monomer composition region, the higher the monomer composition is, the more sensitive the segment length of the same type of monomer is to the minor change in monomer composition. Thus, compared to the synthesis of a compositional gradient, monomer composition should be maintained in a given range and more stringent control over the variation of monomer composition is required for synthesizing a structural gradient.

b. Impact of the Concentration of Nitroxyl Radicals on Segment Lengths. In NM-CRP, nitroxyl radicals work as capping agents. The living chains are capped by nitroxyl radicals and stay dormant during the majority of the reaction, which significantly suppresses termination. A living chain can grow only during the time interval between activation and subsequent deactivation of the same chain (transient lifetime) which is inversely proportional to the concentration of nitroxyl radicals.[38] If the concentration of nitroxyl radicals is too low, the transient lifetime of radicals can be too long to maintain uniform growth of all chains; on the contrary, if the concentration of nitroxyl radicals is too high, the transient lifetime can be too short to allow chains to propagate.

In this work, the concentration of nitroxyl radicals, [SG1], was adjusted by changing the initial amount of unimolecular initiator, BlocBuilder (MS2 compared to MS3) and by adding extra free nitroxyl radicals (MS2 compared to MS4). The monomer sequences of the copolymers synthesized in MS2, MS3, and MS4 are represented by the number-average segment lengths of S and MMA, $N_{n,S}$ and $N_{n,MMA}$, as a function of normalized chain location. As shown in Figure 4, the monomer sequences formed in these three systems are different although other reaction conditions are the same.

The segment lengths of S formed in the very beginning of the reaction, which corresponds to $N_{n,S}$ at a normalized chain location near zero, are significantly different in these three reactions: $N_{n,S}$ of MS2 is 13 units long while the $N_{n,S}$ values of MS3 and MS4 are only six and two units long, respectively, at a normalized chain location near 0. However, the monomer composition is not a governing factor in these systems at the beginning of the reaction when little monomer has been consumed and the monomer compositions are mainly determined by the feed profile and the initial composition in the reactor, which are the same for all three simulation runs. When S is dominant in the reaction mixture, the instantaneous segment lengths of S, $N_{inst,S}$, of MS2 are predicted to be higher than those of MS3 and MS4 under the same monomer compositions as shown in Figure 5, which demonstrates that the formation of segment length in LRP depends not only on the monomer composition but also on the time scale of activation/deactivation cycles.

These three systems differed only by the concentration of nitroxyl radicals. As shown in Figure 6, among these three systems, [SG1] in MS4 is the highest and [SG1] in MS3 is much higher than that of MS2 during the reaction; thus, the transient lifetime of radicals in MS2 is longer than that of MS3 or MS4. Because living chains can propagate only during their transient lifetime, the growth of chains is slowed down with decreasing transient lifetime. In the synthesis of gradient copolymers, monomer composition typically continuously changes as a function of reaction time due to the addition of the second monomer or compositional drift. If the transient lifetime is too short, a segment's growth is

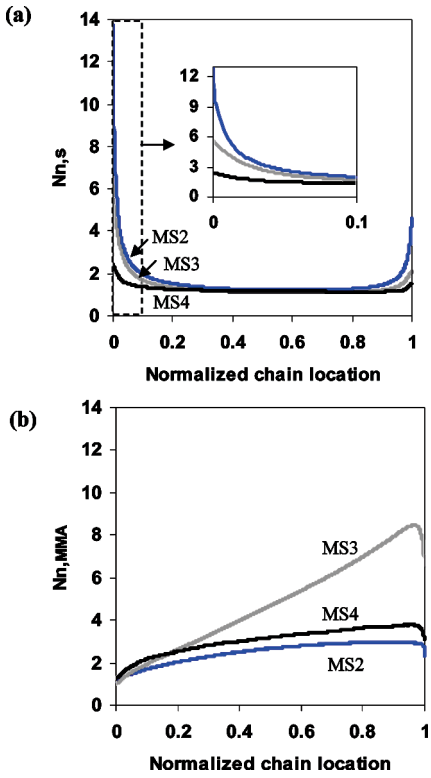

Figure 4. Comparison of monomer sequences formed in MS2, MS3, and MS4: (a) $N_{n,S}$ as a function of normalized chain location. The region of normalized chain location between 0 and 0.1 is amplified and shown separately. (b) $N_{n,MMA}$ as a function of normalized chain location.

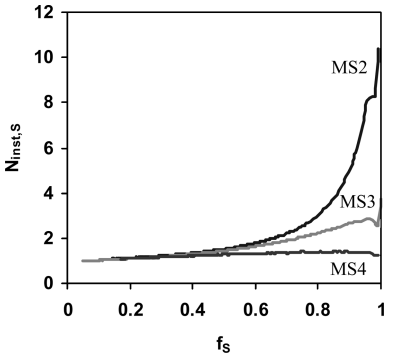

Figure 5. Instantaneous segment length of S, $N_{inst,S}$, as a function of monomer composition of S, f_S, for MS2, MS3, and MS4.

arrested when the chain is capped and rendered dormant. The time interval between deactivation and reactivation of a given chain is on average thousands of seconds long. Thus, when the chain is reactivated, the monomer composition has already changed. Thus, the segment lengths are shorter when the nitroxyl radical concentration is higher.

Long homologous segments are usually formed at the beginning or at the end of the reaction when the reactant mixture is predominantly one monomer. In order to allow segments to develop to fuller lengths, there should be a careful balance between the concentration of nitroxyl radicals and the variation of the monomer composition. If the concentration of nitroxyl radicals is high, the monomer composition should be varied more slowly in order to achieve similar segment lengths.

It should be noted that the concentration of nitroxyl radicals is closely related to the livingness of the reaction,

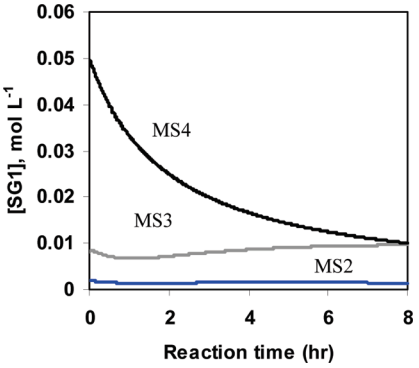

Figure 6. Concentration of nitroxyl radicals, [SG1], as a function of reaction time for MS2, MS3, and MS4.

i.e., the fraction of dead polymer formed in the reaction system, which can significantly affect the monomer sequence if combination is the favored termination mode. In combination, two radical chains with similar tail sequences are combined, which leads to a sequence axis of symmetry, that is, chains that are styrene-rich at both ends, and causes a dramatic increase in the average segment length near the tail of chains, as shown in Figure 4. In fact, the monomer sequence can be sensitive to many factors. For example, the variation of the initial amount of unimolecular initiator can affect the profile of monomer composition during the reaction and thus affect the segment length formed during the reaction. As shown in Figure 4 b, $N_{n,MMA}$ of MS3 is higher than those of MS2 and MS4 at the tail of chains, while $N_{n,S}$ of MS3 is between that of MS2 and MS4 at the head of chains. This is because the initial concentration of unimolecular initiator in MS3 is 10 times higher than that in MS2 or MS4, and this leads to a different monomer composition at the end of the reaction.

Formation of Sequences along Gradient Copolymer Chains. The most attractive and unique feature of gradient copolymers is well-defined microscopic monomer sequences in which segment lengths vary along the copolymer chains according to a predesigned pattern. As discussed in the previous section, a structural gradient can be formed in S/MMA copolymerization only if the monomer composition strongly favors one type of monomer. Since f_{MMA} needs to be relatively high in order to form a structural gradient of MMA, extra free nitroxyl radicals are necessary for controlling the reaction as living. Thus, the profiles of monomer composition and nitroxyl radical concentration during the reaction are the keys to achieve a well-defined microstructure along the chains.

Theoretically, there are an infinite number of different feed profiles of monomer and free nitroxyl radicals that can be utilized in forced gradient copolymerization. In fact, however, the majority of the gradient copolymers that have been reported in the literature were synthesized using a constant feed profile of the second monomer, in which the feed rate of the second monomer is maintained as a constant during the reaction. In the reactions involving a large proportion of a methacrylic ester, the free nitroxyl radicals were usually added all at once in the very beginning of the reaction. Thus, we first investigated the monomer sequences generated by the feed profiles that are most widely used in the current syntheses of gradient copolymers. On the basis of these observations, methods to optimize the feed profiles of monomer and nitroxyl radicals to achieve a better structural gradient are proposed.

a. Impact of Feed Profile of Nitroxyl Radicals on Sequences. The free nitroxyl radicals are typically added into

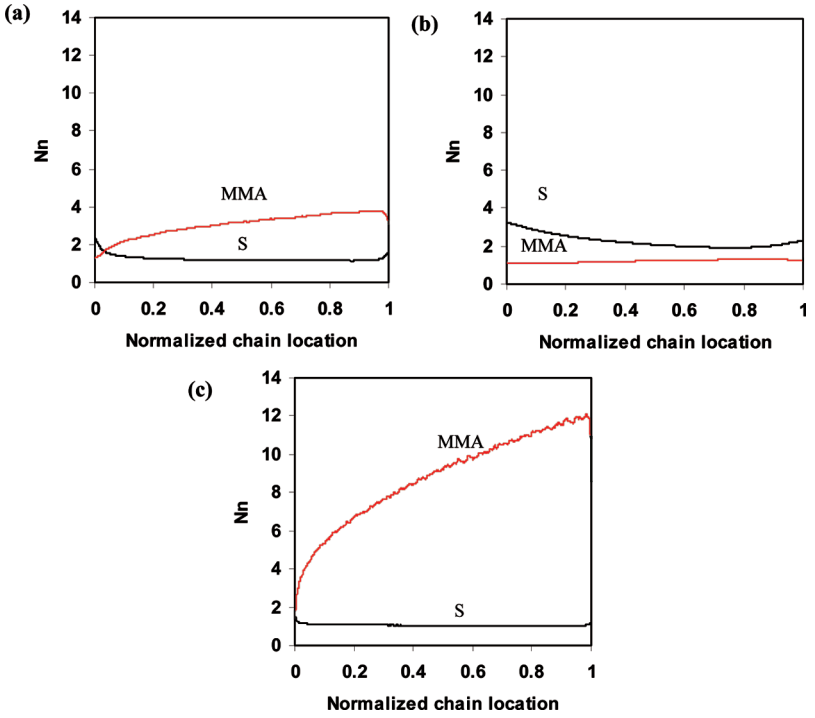

Figure 7. $N_{n,S}$ and $N_{n,MMA}$ as a function of normalized chain location: (a) MS4, (b) MS5, and (c) MS6.

the reaction system in the very beginning of the reaction. With such a feed profile, the concentration of nitroxyl radicals normally decreases as reaction proceeds because the total volume of the reaction system continues to increase due to the addition of the second monomer. Under this circumstance, the transient lifetime of propagating radicals is quite short in the beginning of the reaction which may prohibit segments near the head of the chains from being fully developed. This is because in the very beginning of the reaction when long segments of S are formed, the growth of the S segments is slow because of the short transient lifetime, and f_S plummets quickly after the start of the reaction due to the continuous addition of MMA monomer, which limits the growth of homologous segments of S. For instance, $N_{n,S}$ is only two units long near the head of chains in MS4.

Given this feed profile of nitroxyl radicals, is it possible to achieve a more pronounced structural gradient by changing the constant feed rate of monomer? In order to answer this question, we decreased the feed rate of MMA to one-fifth of that in MS4, and the modified recipe is referred to as MS5. Parts a and b of Figure 7 show the number-average segment lengths along the chains in MS4 and MS5, respectively. The $N_{n,S}$ value near the head of the chains is three units long in MS5 which is only a little longer than that in MS4. However, there is almost no structural gradient of MMA in monomer sequences in MS5, in which $N_{n,MMA}$ is about one unit long throughout the chain. The next scenario tested was an increase in the feed rate of MMA in order to improve the structural gradient of the MMA segments. This recipe is designated as MS6, and the $N_{n,S}$ and $N_{n,MMA}$ values as a function of normalized chain location are plotted in Figure 7c. The S segments near the head of the chains become even shorter than those in MS4. In addition, the nitroxyl radical concentration may be too low to control the reaction as living in the later stage of the reaction if a large amount of MMA is added into the system. Taking all these considerations into account, our results indicate that the addition of free nitroxyl radicals all at once in the beginning of the reaction is not an optimal feed profile for preparing structural gradient copolymers.

As an alternative, we propose the addition of free nitroxyl radical together with MMA monomer into the reaction system, which can also be easily operated in syntheses in practice. With this feed profile, the nitroxyl radical concentration increases with an increasing proportion of MMA in the system. In this way, the growth of long segments of S will not be limited when f_{MMA} is low, and the reaction can still be controlled as living when f_{MMA} is high. As an example, the feed profiles of SG1 in MS4 and MS6 were modified by adding 0.2 mol % SG1 of the feed rate of MMA continuously into the reaction, and the modified recipes are referred to as MS7 and MS1. As shown in Figure 8a,c, $N_{n,S}$ near the head of the chains in MS7 and MS1 is 11 units long and 7 units long, respectively, which is much longer than that in MS4 or MS6.

b. Impact of Constant Feed Profile of Monomers on Sequences. The simulation runs MS7, MS8, and MS1 differed by the constant feed rate of MMA only. Figure 8 shows the number-average segment lengths as a function of normalized chain location resulting from these three recipes. It is obvious that the segment lengths of MMA at the same normalized chain location increase with increasing feed rate of MMA. In MS7, $N_{n,MMA}$ is only four units long at the tail of the chains. In MS8, where the feed rate of MMA is double that in MS7, $N_{n,MMA}$ is increased to seven units long at the tail of the chains. In MS1 where the feed rate of MMA is further increased to 3 times higher than that in MS7, $N_{n,MMA}$ is increased to 11 units long at the tail of the chains. By increasing the feed rate, MMA segments grow longer which leads to a more pronounced gradient of MMA along the chain. However, by doing so, the segment lengths of S plummet more quickly at the head of the chain which leads to monomer sequences comprised of MMA segments with increasing lengths along the copolymer chain with only one unit long S segments embedded in them. Under these circumstances, the copolymer composition favors the type of monomer fed into the system more as the reaction continues,

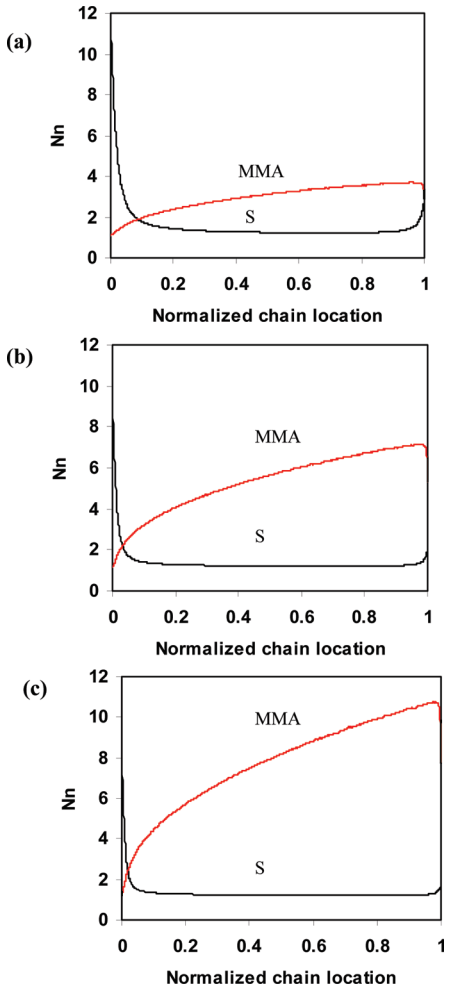

Figure 8. $N_{n,S}$ and $N_{n,MMA}$ as a function of normalized chain location: (a) MS7, (b) MS8, and (c) MS1.

and the copolymers can finally be turned into nearly pure homopolymers.

As discussed above, a structural gradient can only be formed when the monomer composition strongly favors one type of monomer. Figure 9 shows the variation of f_{MMA} during the reactions of MS7, MS8, and MS1. The regions of f_{MMA} where segment lengths can be varied efficiently by changing monomer composition are marked by the shadowed portion. In MS7, f_{MMA} does not increase above 0.8 until 6 h of reaction and reaches only 0.85 at the end of the reaction. Compared to MS7, the increase of f_{MMA} is much faster in the other two recipes, where f_{MMA} increased above 0.8 after 3 h in MS8 and 2 h in MS1. On the other hand, however, f_S plummets much faster with an increasing feed rate of MMA. For instance, f_S decreased below 0.5 after only 0.55 h of reaction in MS1. Because of the quick decrease of f_S, there is insufficient time to develop a structural gradient of the S segments. Therefore, only a "partial" structural gradient, in which the segment lengths of only one type of monomer vary along the copolymer chains, can be achieved by increasing the constant feed rate of the second monomer.

If it is still desired to maintain a constant feed profile of monomer, the other possible solution to achieve a structural gradient of both types of monomer is to lower the feed rate of the second monomer and elongate the reaction time. By doing so, long segments of both types of monomer can be developed at both ends of the chain, but there will inevitably be a long region between the two ends representing a random

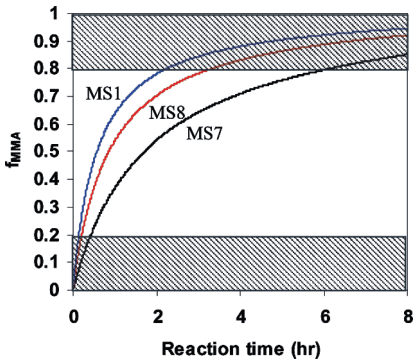

Figure 9. f_{MMA} as a function of reaction time for MS7, MS8, and MS1, in which the monomer composition regions where segment lengths can be varied efficiently by changing the monomer composition are shaded.

copolymer where the segment lengths of both MMA and S are very short. Although it has been most widely used, a constant feed profile of the second monomer is not optimal to prepare structural gradient copolymers.

On the basis of these observations, in order to form an "ideal" structural gradient for S/MMA comonomer pairs as depicted in Scheme 1, the monomer composition in the reactant mixture should be predominantly one type of monomer during most of the reaction time, and a quick transition from high f_S to high f_{MMA} is needed. According to these requirements, a variable feed profile, in which the feed rate of the second monomer changes during the reaction, is a better choice than a constant feed profile to prepare S/MMA structural gradient copolymers. For instance, in the early stage of the reaction, the feed rate of MMA should be relatively low to allow for the formation of the structural gradient of the S segments. Then, in the middle of the reaction, f_{MMA} has to be quickly increased above 0.8 as soon as f_S drops below 0.8 in order to avoid incorporating random copolymer sequences into the chains, which requires a sudden introduction of a large amount of MMA into the reaction system. After the monomer composition is changed to predominantly MMA, the feed rate of MMA needs to be adjusted again in order to achieve a structural gradient of MMA segments.

To demonstrate that these approaches do indeed create a more "ideal" structural gradient, we modified the feed profile of MMA monomer according to these ideas as an example, and the modified recipe is referred to as MS9. In MS9, the feed rate of MMA was low in the early stage of reaction, which allows f_S to decrease slowly within the range where a structural gradient of S can be generated. The transition from an S-dominant to an MMA-dominant reaction mixture was rendered fast by introducing a large amount of MMA in the middle of the reaction in order to avoid producing random monomer sequences. During the later stage of reaction, MMA is dominant and f_{MMA} was gradually increased, which allows for the formation of a smooth structural gradient of MMA. Figure 10 shows the monomer sequences generated in MS9. Compared to monomer sequences generated by constant feed profiles (MS7, MS8, and MS1), the variable feed profile in MS9, which can also be applied in synthesis in a facile way in practice, clearly generates more pronounced and smoother structural gradients of both S and MMA along the chains.

Factors Affecting the Polydispersity of Monomer Sequences along Copolymer Chains. Next, the KMC simulations were used to assess the factors that affect the uniformity of monomer sequences along copolymer chains.

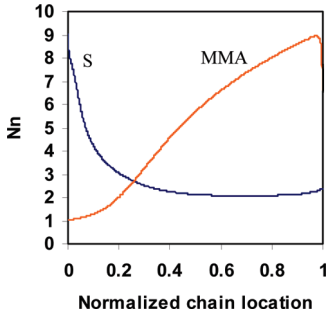

Figure 10. $N_{n,S}$ and $N_{n,MMA}$ as a function of normalized chain location for MS9.

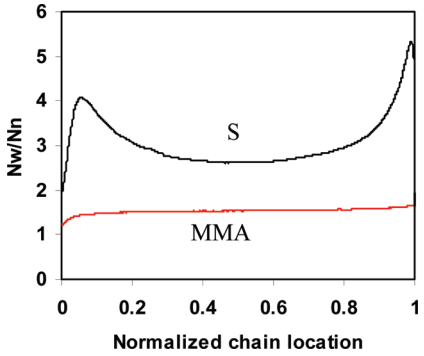

Figure 11. Segment PDI, N_w/N_n, of MMA and S segments as a function of normalized chain location in MS7.

High uniformity of sequence patterns would be preferred in order to clearly unravel the impact of a given microscopic monomer sequence on macroscopic material properties. The traditional polydispersity index of molecular weight (molecular weight PDI) cannot provide any direct information about the reproducibility of sequences formed on different chains, since copolymer chains with the same molecular weight can have quite different sequences along the chain. In order to express the polydispersity of monomer sequences formed in different chains of the whole population, we recorded the polydispersity index of local segment lengths (segment PDI) along the copolymer chains using KMC simulations using MS7 as a baseline for comparison. As shown in Figure 11, the local segment PDI of S in MS7 has two maxima indicating broad distributions of segment lengths near both ends of the chains. Compared to S segments, the segment PDI of MMA is much lower. This is because only very short segments of MMA were formed during the majority of the reaction, and f_{MMA} was not very high even at the end of the reaction.

The factors that result in a high segment PDI of S were first investigated. Because MMA monomer was fed into a pure S monomer environment, f_S is quite high (above 0.95) in the very beginning of the reaction. With such a high f_S value, it is possible to form relatively long segments of S if the transient lifetime of radicals is long enough. However, f_S decreases so quickly in the reaction system, and only a small portion of chains can be activated at a given moment. As a result, S segments with various lengths were formed at the head of the chains, which is manifested by a maximum near the head of the chains.

In addition, termination can also significantly affect the uniformity of monomer sequences. In MS7, the major termination mode is combination, in which two radical chains are combined tail-to-tail to form a symmetric structure. This

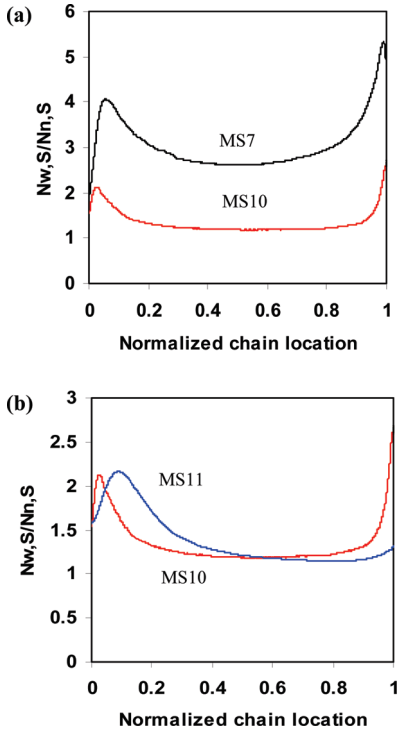

Figure 12. Comparison of $N_{w,S}/N_{n,S}$ as a function of normalized chain location: (a) MS7 and MS10; (b) MS10 and MS11.

symmetric structure of dead polymer terminated by combination is in stark contrast to the structure of other chains, which can greatly increase the segment PDI near the tails of the chains.

Therefore, the chains need to grow more uniformly when long segments are formed, and termination should be reduced in order to achieve a narrow distribution of monomer sequences in the whole population. On the basis of these findings related to the polydispersity of monomer sequence, we modified the nitroxyl radical feed profile in MS7 as an example to demonstrate how to optimize the polydispersity of monomer sequence. First of all, in order to make chains grow more uniformly in the early stage of the reaction, 0.004 mol L^{-1} SG1 was introduced to the initial feed in the reactor, and the modified recipe is referred to as MS10. With extra free SG1, the time interval between reactivation and deactivation is shortened, and thus segments grow more uniformly. The segment PDI as a function of normalized chain location resulting from MS10 is plotted together with that from MS7 for comparison purposes, as shown in Figure 12a. The value of $N_{w,S}/N_{n,S}$ of MS10 is much lower than that of MS7 at all normalized chain locations. However, $N_{w,S}/N_{n,S}$ still has an upward bend at the tail of the chains, indicating the existence of a certain portion of dead polymers terminated by combination. In order to further suppress termination, the concentration of nitroxyl radical needs to be increased in the later stage of the reaction. For this reason, the feed rate of SG1 in MS10 was increased by 2.5 times, and the modified reaction recipe is referred to as MS11. As shown in Figure 11b, after these adjustments, the segment PDI of S is decreased below two for the majority of the normalized chain length. The monomer sequences resulting from MS11 are similar to those from MS7, except that the number-average segment lengths of S near the head of the chains in MS11 are slightly shorter than those in MS7.

Compared to molecular weight PDI, it is much harder to maintain segment PDI low everywhere along the copolymer

chains. Because segment PDI depends on the entire growth histories of individual chains, the chains have to grow highly uniformly throughout the reaction. In order to achieve a low polydispersity of monomer sequences, the reaction conditions need to be carefully tuned throughout the reaction. Segment PDI can be tuned by multiple factors, such as nitroxyl radical concentration and monomer feed rate. However, it should be noted that many of these factors can also change the sequences along the chain. Thus, the reaction conditions need to be carefully balanced in order to achieve a targeted chain sequence as well as a reasonably low polydispersity of chain sequence.

Conclusions

The impact of different synthesis conditions on monomer sequences was investigated by KMC simulations for S/MMA forced gradient copolymerization with NM-CRP. It was shown that segment lengths increase exponentially with increasing monomer composition for both S and MMA. For this reason, segments with more than four units long can be formed only if the monomer composition highly favors the same type of monomer. In addition, the concentration of nitroxyl radicals can also affect the length of segments. If the concentration of nitroxyl radicals is too high, the growth of a long segment can be arrested by deactivation before it is fully developed. Thus, the monomer sequences along the copolymer chain are mainly determined by the feed profile of monomer as well as that of nitroxyl radicals during the reaction. It was found that a constant feed profile of monomer, which is widely used in current syntheses of gradient copolymers, is actually not suitable to make structural gradient copolymers. Through our KMC simulations, it is suggested that a variable feed profile of monomer is a better choice to make structural gradient copolymers. Furthermore, it was found that only short segments can be formed near the head of the chains if free nitroxyl radicals are added to the system all at once at the beginning of the reaction. On the basis of these findings, a new feed profile of free nitroxyl radicals, which can generate a more pronounced structural gradient along the chains, was proposed.

The factors affecting the uniformity of monomer sequences along the chain were also investigated. It was found that segment PDI can be significantly affected by the uniformity of chain growth when monomer composition highly favors one type of monomer. In addition, termination by combination can also play an important role in the polydispersity of monomer sequences along the chain. It was shown through a case study that the uniformity of monomer sequences can be efficiently improved by increasing the uniformity of chain growth in the initial phase and reducing termination in the later stage of the reaction.

It should be noted that more than one aspect of sequence can be changed when a single reaction condition is adjusted, since these factors have multiple impacts on chain sequence. To deal with this complex system, it is necessary to employ "programmed" syntheses where a recipe is designed by computational methods in advance. KMC simulations offer a powerful tool to predict the appropriate synthesis recipe for generating this kind of well-defined microstructure. Further studies to this end are underway.

Acknowledgment. This work was supported by the MRSEC program of the National Science Foundation (DMR-0520513) at the Materials Research Center of Northwestern University.

References and Notes

(1) Nicolas, J.; Dire, C.; Mueller, L.; Belleney, J.; Charleux, B.; Marque, S. R. A.; Bertin, D.; Magnet, S.; Couvreur, L. *Macromolecules* **2006**, *39*, 8274–8282.
(2) Bates, F. S.; Fredrickson, G. H. *Phys. Today* **1999**, *52*, 32–38.
(3) Beginn, U. *Colloid Polym. Sci.* **2008**, *286*, 1465–1474.
(4) Pakula, T.; Matyjaszewski, K. *Macromol. Theory Simul.* **1996**, *5*, 987–1006.
(5) Matyjaszewski, K.; Ziegler, M. J.; Arehart, S. V.; Greszta, D.; Pakula, T. *J. Phys. Org. Chem.* **2000**, *13*, 775–786.
(6) Lefebvre, M. D.; Olvera de la Cruz, M.; Shull, K. R. *Macromolecules* **2004**, *37*, 1118–1123.
(7) Kim, J.; Zhou, H.; Nguyen, S. T.; Torkelson, J. M. *Polymer* **2006**, *47*, 5799–5809.
(8) Shull, K. R. *Macromolecules* **2002**, *35*, 8631–8639.
(9) Gorman, C. B.; Petrie, R. J.; Genzer, J. *Macromolecules* **2008**, *41*, 4856–4865.
(10) Jiang, R.; Jin, Q.; Li, B.; Ding, D.; Wickham, R. A.; Shi, A. C. *Macromolecules* **2008**, *41*, 5457–5465.
(11) Wang, R.; Li, W.; Luo, Y.; Li, B.; Shi, A.; Zhu, S. *Macromolecules* **2009**, *42*, 2275–2285.
(12) Dotson, N. A.; Galvan, R.; Laurence, R. L.; Tirrell, M. *Polymerization Process Modeling*; VCH Publishers Inc.: New York, 1995.
(13) Mignard, E.; Lablanc, T.; Bertin, D.; Guerret, O.; Reed, W. F. *Macromolecules* **2004**, *37*, 966–975.
(14) Dettmer, C. M.; Gray, M. K.; Torkelson, J. M.; Nguyen, S. T. *Macromolecules* **2004**, *37*, 5504–5512.
(15) Min, K.; Oh, J. K.; Matyjaszewski, K. *J. Polym. Sci., Part A: Polym. Chem.* **2007**, *45*, 1413–1423.
(16) Mok, M. M.; Pujari, S.; Burghardt, W. R.; Dettmer, C. M.; Nguyen, S. T.; Ellison, C. J.; Torkelson, J. M. *Macromolecules* **2008**, *41*, 5818–5829.
(17) Wang, R.; Luo, Y.; Li, B.; Sun, X.; Zhu, S. *Macromol. Theory Simul.* **2006**, *15*, 356–368.
(18) Sun, X.; Luo, Y.; Wang, R.; Li, B.; Liu, B.; Zhu, S. *Macromolecules* **2007**, *40*, 849–859.
(19) Beginn, U. *Polymer* **2006**, *47*, 6880–6894.
(20) Fujisawa, T.; Penlidis, A. *J. Macromol. Sci., Part A: Pure Appl. Chem.* **2008**, *45*, 115–132.
(21) Wang, L.; Broadbelt, L. J. *Macromolecules* **2009**, DOI: 10.1021/ma901298h.
(22) Gillespie, D. T. *J. Comput. Sci.* **1976**, *22*, 403–434.
(23) Tabash, R. Y.; Teymour, F. A.; Debling, J. A. *Macromolecules* **2006**, *39*, 829–843.
(24) Bertin, D.; Gigmes, D.; Marque, S. R. A.; Tordo, P. *Macromolecules* **2005**, *38*, 2638–2650.
(25) Fischer, H.; Radom, L. *Angew. Chem., Int. Ed.* **2001**, *40*, 1340–1371.
(26) Campbell, J. D.; Teymour, F.; Morbidelli, M. *Macromolecules* **2003**, *36*, 5491–5501.
(27) Beuermann, S.; Buback, M.; Davis, T. P.; Gilbert, R. G.; Hutchinson, R. A.; Olaj, O. F.; Russell, G. T.; Schweer, J.; Van Herk, A. M. *Macromol. Chem. Phys.* **1997**, *198*, 1545–1560.
(28) Buback, M.; Kuchta, F. D. *Macromol. Chem. Phys.* **1997**, *198*, 1455–1480.
(29) Brandrup, J.; Immergut, E. H.; Grulke, E. A. *Polymer Handbook*, 4th ed.; Wiley: New York, 1999.
(30) Moad, G.; Solomon, D. H. *The Chemistry of Free Radical Polymerization*; Elsevier Science: New York, 1995.
(31) Cho, A. S. Mechanistic Modeling of Nitroxide-Mediated Controlled Radical Polymerization. Ph.D. Thesis, Northwestern University, **2009**.
(32) Meyer, T.; Keurentjes, J. *Handbook of Polymer Reaction Engineering*; Wiley-VCH: New York, 2005.
(33) Hui, A. W.; Hamielec, A. E. *J. Appl. Polym. Sci.* **1972**, *16*, 749–769.
(34) Sobek, J.; Martschke, R.; Fischer, H. *J. Am. Chem. Soc.* **2001**, *123*, 2849–2857.
(35) Guillaneuf, Y.; Gigmes, D.; Marque, S. R. A.; Tordo, P.; Bertin, D. *Macromol. Chem. Phys.* **2006**, *207*, 1278–1288.
(36) Guillaneuf, Y.; Bertin, D.; Castigolles, P.; Charleux, B. *Macromolecules* **2005**, *38*, 4638–4646.
(37) Fukuda, T.; Ma, Y.-D.; Inagaki, H. *Macromolecules* **1984**, *18*, 17–26.
(38) Goto, A.; Fukuda, T. *Prog. Polym. Sci.* **2004**, *29*, 329–385.